A cell-centered implicit-explicit Lagrangian scheme for a unified model of nonlinear continuum mechanics on unstructured meshes

Walter Boscheri

walter.boscheri@unife.it

University of Ferrara (Italy)

- Department of Mathematics and Computer Science -

22^{nd} February 2023 - PRIN 2017 Final Workshop

Outline

Outline

Lagrangian methods

$$\frac{D}{Dt}() = \frac{\partial}{\partial t}() + \overline{\mathbf{v}}\,\nabla()$$

J. Von Neumann, R. D. Richtmyer. A method for the numerical calculation of hydrodynamic shocks. *J. Applied Physics* 21 (1950) 232-237.

Advantages

- availability of trajectory information;
- less numerical diffusion;
- material interfaces are precisely located and identified.

Lagrangian methods

$$\frac{D}{Dt}() = \frac{\partial}{\partial t}() + \overline{\mathbf{v}}\,\nabla()$$

J. Von Neumann, R. D. Richtmyer. A method for the numerical calculation of hydrodynamic shocks.*J. Applied Physics* 21 (1950) 232-237.

Advantages

- availability of trajectory information;
- less numerical diffusion;
- material interfaces are precisely located and identified.

Disadvantages

- high computational cost;
- mesh distortion.

Lagrangian methods (brief overview)

Cell-centered finite volume schemes for hydrodynamics

C.D. Munz. On Godunov-type schemes for Lagrangian gas dynamics.
SIAM Journal on Numerical Analysis 31 (1994) 17-42.

B. Després, C. Mazeran. Symmetrization of Lagrangian gas dynamic in dimension two and multimdimensional solvers.
C.R. Mecanique 331 (2003) 475-480.

B. Després, C. Mazeran. Lagrangian gas dynamics in two dimensions and Lagrangian systems.
ARMA 178 (2005) 327-372.

P.H. Maire. A high-order cell-centered Lagrangian scheme for two-dimensional compressible fluid flows on unstructured meshes.
J. Comput. Phys. 228 (2009) 2391-2425.

P.-H. Maire, R. Abgrall, J. Breil, J. Ovadia. A cell-centered Lagrangian scheme for two-dimensional compressible flow problems.
SIAM SISC 29 (2007) 1781-1824.

Lagrangian methods (brief overview)

Finite element schemes for solid mechanics

D. P. Flanagan, T. Belytschko. A uniform strain hexahedron and quadrilateral with orthogonal hourglass control.
IJNME 17 (1981) 679-706.

G.L. Goudreau, J.O. Hallquist. Recent developments in large-scale finite element Lagrangian hydrocode technology.
CMAME 33 (1982) 725-757.

G. Scovazzi, B. Carnes, X. Zeng, S. Rossi. A simple, stable, and accurate linear tetrahedral finite element for transient, nearly, and fully incompressible solid dynamics: a dynamic variational multiscale approach.
IJNME 106 (2016) 799-839.

Lagrangian methods (brief overview)

Finite volume schemes for solid mechanics

J.A. Trangenstein and P. Colella. A higher-order Godunov method for modeling finite deformation in elastic-plastic solids.
Communications on Pure and Applied Mathematics 44 (1991) 41-100.

G. Kluth, B. Després. Discretization of hyperelasticity on unstructured mesh with a cell-centered Lagrangian scheme.
JCP 229 (2010) 9092-9118.

J. Bonet, A. J. Gil, C. Hean Lee, M. Aguirre, R. Ortigosa. A first order hyperbolic framework for large strain computational solid dynamics. part I: Total Lagrangian isothermal elasticity.
CMAME 283 (2015) 689-732.

A. J. Gil, C. Hean Lee, J. Bonet, and R. Ortigosa. A first order hyperbolic framework for large strain computational solid dynamics. part II: Total Lagrangian compressible, nearly incompressible and truly incompressible elasticity.
CMAME 300 (2016) 146-181.

Outline

Updated Lagrangian framework

Lagrange-Euler mapping

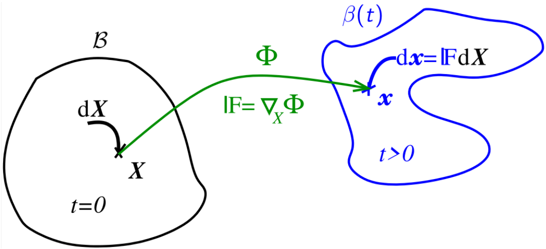

Figure: Lagrange-Euler mapping $\mathbf{\Phi}$ relating a material Lagrangian point $\boldsymbol{X}$ at $t = 0$ and a spatial Eulerian one $\boldsymbol{x}$ at $t > 0$.

$\mathcal{B} \longrightarrow \beta(t)$	Computational domain
$\boldsymbol{X} \longmapsto \boldsymbol{x} = \mathbf{\Phi}(\boldsymbol{X}, t)$	Lagrange-Euler mapping
$\mathbb{F}(\boldsymbol{X}, t) = \nabla_X \mathbf{\Phi}(\boldsymbol{X}, t)$	Deformation gradient
$J(\boldsymbol{X}, t) = \det\left(\mathbb{F}(\boldsymbol{X}, t)\right)$ s.t. $J(\boldsymbol{X}, t = 0) = 1$	Determinant of $\mathbb{F}$

Updated Lagrangian framework

Measures of deformation

Decomposition of the total deformation gradient: $\mathbb{F} = \mathbb{F}_e \mathbb{F}_p$

Effective elastic distortion: $\mathbb{A}_e = \mathbb{F}_e^{-1}$

Infinitesimal frame $\mathbb{A}_e$ (local basis triad) that characterizes deformation and orientation of the material particles.

Compatibility condition: $\nabla \times \mathbb{A}_e = 0$

Metric tensor: $\mathbb{G}_e = \mathbb{A}_e^{\mathsf{T}} \mathbb{A}_e$

Deviatoric part: $\mathring{\mathbb{G}}_e = \mathbb{G}_e - \frac{1}{3}\mathrm{tr}(\mathbb{G}_e)\mathbb{I}$

Nonlinear (quadratic) compatibility condition.

The Godunov-Peshkov-Romenski (GPR) model

(I. Peshkvo and E. Romenski. Cont. Mech. Therm. 2016)

Physical variables: $\mathbf{Q} := \{\omega, \mathbf{v}, E, \mathbf{J}, \mathbb{G}_e\}$

$$\rho \frac{\mathrm{d}\omega}{\mathrm{d}\,t} - \nabla \cdot \mathbf{v} = 0, \tag{1a}$$

$$\rho \frac{\mathrm{d}\mathbf{v}}{\mathrm{d}\,t} - \nabla \cdot \mathbb{T} = \mathbf{0}, \tag{1b}$$

$$\rho \frac{\mathrm{d}E}{\mathrm{d}\,t} - \nabla \cdot (\mathbb{T}\mathbf{v}) + \nabla \cdot \mathbf{q} = 0, \tag{1c}$$

$$\rho \frac{\mathrm{d}\mathbf{J}}{\mathrm{d}\,t} + \nabla\theta = -\frac{\rho\mathbf{H}}{\Psi}, \tag{1d}$$

$$\frac{\mathrm{d}\mathbb{G}_e}{\mathrm{d}\,t} + \mathbb{G}_e\nabla\mathbf{v} + \nabla\mathbf{v}^{\top}\mathbb{G}_e = \frac{2}{\rho\Theta}\sigma, \tag{1e}$$

Notation

ρ	mass density	$\omega = \rho^{-1}$	specific volume
$\mathbf{v} = (u, v, w)$	velocity vector	$\mathbb{T}$	Cauchy stress tensor
$E(\rho, p, \mathbf{v}, \mathbb{G}_e)$	total energy	$\mathbf{J}$	thermal impulse

Energy and Cauchy stress

Total energy: $E = E_h(\rho, p) + E_e(\mathbb{G}_e) + E_{th}(\mathbf{J}) + E_k(\mathbf{v})$

$$E_h = \varepsilon(\rho, p) \qquad E_e = \frac{c_{\mathrm{sh}}^2}{4}\|\mathring{\mathbb{G}}_e\|^2 \qquad E_{th} = \frac{1}{2}\alpha^2\|\mathbf{J}\|^2 \qquad E_k = \frac{1}{2}\|\mathbf{v}\|^2$$

Cauchy stress tensor: $\mathbb{T} = -p\mathbb{I} + \boldsymbol{\sigma}$

Pressure (hydrodynamic energy): p

Tangential stress: $\boldsymbol{\sigma} = -2\rho\mathbb{G}_e\dfrac{\partial E}{\partial \mathbb{G}_e} = -\rho c_{\mathrm{sh}}^2\mathbb{G}_e\mathring{\mathbb{G}}_e$

Remark. The spherical part of $\boldsymbol{\sigma}$ for our choice of the elastic energy is not zero but scales as $\sim \|\mathring{\mathbb{G}}_e\|^2$

Equation of state (EOS) for E_h

- ideal gas EOS

$$\varepsilon(\rho, p) = \frac{p}{\rho(\gamma - 1)}, \qquad \theta = \frac{\varepsilon}{c_v}, \qquad c_0^2 = \frac{\gamma p}{\rho},$$

- Mie-Grüneisen EOS

$$\varepsilon(\rho, p) = \frac{p - \rho_0 c_0^2 f(J)}{\rho_0 \Gamma_0}, \qquad f(J) = \frac{(J-1)(J - \frac{1}{2}\Gamma_0(J-1))}{(J - s(J-1))^2},$$

with $J = \frac{\rho}{\rho_0}$.

- Neo-Hookean hyperelastic EOS

$$\varepsilon(\rho, p) = \frac{G}{4\rho_0}\left((J-1)^2 + (\log(J))^2\right), \qquad p = -\frac{G}{2}\left(J - 1 + \frac{\log(J)}{J}\right),$$

where $G = \rho_0 c_{\mathrm{sh}}^2$ is the shear modulus.

Closure for inelastic deformations and fluid flows

Relaxation function in the source term for $\mathbb{G}_e$

$$\Theta = \tau_1 \frac{c_{\mathrm{sh}}^2}{3} |\mathbb{G}_e|^{-5/6}$$

$|\mathbb{G}_e| = \det(\mathbb{G}_e)$ and τ_1 is the strain relaxation time.

fluids $\rightarrow$ $\tau_1 = \frac{6\mu}{\rho_0 c_s^2}$ — μ: dynamic viscosity coefficient

solids $\rightarrow$ $\tau_1 = \tau_1 = \tau_{10} \left(\frac{\sigma_Y}{\sigma}\right)^n$ — τ_{10}, n: material parameters, σ_Y: Yield stress

$$\sigma = \sqrt{\frac{3}{2}\mathrm{tr}(\mathring{\sigma}^2)}, \qquad \mathring{\sigma} = \boldsymbol{\sigma} - \frac{1}{3}\mathrm{tr}(\boldsymbol{\sigma})\mathbb{I}$$

solids		fluids	
$\tau_1 = \infty$	elastic solids	$0 < \tau_1 < \infty$, $\sigma_0 = 0$	viscous fluids
$0 < \tau_1(\sigma_0) < \infty$	elastoplastic solids	$\tau_1 = 0$, $\sigma_0 = 0$	ideal fluids

Heat conduction

Relaxation function in the source term for $\mathbf{J}$

$$\Psi = \alpha^2 \tau_{20} \tau_2, \qquad \tau_{20} = \frac{\rho}{\rho_0} \frac{\theta_0}{\theta},$$

Consistency with second law of thermodynamics:

$$\mathbf{q} = \theta \mathbf{H} = \alpha^2 \theta \mathbf{J}, \qquad \mathbf{H} := \frac{\partial E}{\partial \mathbf{J}} = \alpha^2 \mathbf{J}.$$

Thermal perturbation propagation speed: $c_\mathrm{h}^2 = \frac{\alpha^2}{\rho_0^2} \frac{\theta}{c_v}$

Effective heat conductivity: $\kappa = \tau_2 \alpha^2 \frac{\theta_0}{\rho_0} \Rightarrow$ **Fourier law:** $\mathbf{q} = -\kappa \nabla \theta$

Notation

- τ_2 thermal relaxation time
- θ temperature
- α parameter related to the thermal propagation speed

Outline

Computational mesh and data representation

Unstructured grid composed of triangles or tetrahedra

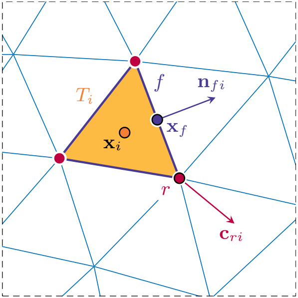

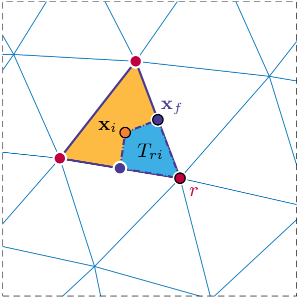

Corner vector: $\mathbf{c}_{ri} = \frac{1}{d} \sum_{f \in \mathcal{F}_{ri}} s_f \mathbf{n}_{fi}$ such that $\sum_{r \in \mathcal{R}_i} \mathbf{c}_{ri} = 0$

Cell mass: $m_i := \int_{T_i(t)} \rho \, \mathrm{d}\mathbf{x}$

Cell average: $\phi_i = \frac{1}{m_i} \int_{T_i(t)} \rho \phi \, \mathrm{d}\mathbf{x}$

Fully discrete finite volume scheme

Physical balance laws IMplicit-EXplicit time discretization

$$\omega_i^{n+1} = \omega_i^n + \frac{\Delta t}{m_i} \sum_{r \in \mathcal{R}_i} \tilde{\mathbf{v}}_r^* \cdot \frac{1}{6} \left(\mathbf{c}_{ri}^n + 4\mathbf{c}_{ri}^{n+1/2} + \mathbf{c}_{ri}^{n+1} \right), \tag{2a}$$

$$\mathbf{v}_i^{n+1} = \mathbf{v}_i^n + \frac{\Delta t}{m_i} \sum_{r \in \mathcal{R}_i} \tilde{\boldsymbol{f}}_{ri}^*, \tag{2b}$$

$$E_i^{n+1} = E_i^n + \frac{\Delta t}{m_i} \left[\sum_{r \in \mathcal{R}_i} \tilde{\boldsymbol{f}}_{ri}^* \cdot \tilde{\mathbf{v}}_r^* + \sum_{f \in \mathcal{F}_i} \widehat{\mathbf{q}_{fi} \cdot \mathbf{n}_{fi}}^{\,n} s_f^n \right] = 0, \tag{2c}$$

$$\mathbf{J}_i^{n+1} = \mathbf{J}_i^n - \frac{\Delta t}{m_i} \sum_{f \in \mathcal{F}_i} \widehat{\theta_{fi} \mathbb{I} \cdot \mathbf{n}_{fi}}^{\,n} s_f^n - \Delta t \frac{\mathbf{H}_i^{n+1}}{\Psi_i^{n+1}}, \tag{2d}$$

$$\mathbb{G}_{e_i}^{n+1} = \mathbb{G}_{e_i}^n - \Delta t \left(\mathbb{G}_{e_i}^n \, \mathbb{L}_i(\tilde{\mathbf{v}}^*) + \mathbb{L}_i(\tilde{\mathbf{v}}^*)^\intercal \, \mathbb{G}_{e_i}^n \right) + \Delta t \frac{2\boldsymbol{\sigma}_i^{n+1}}{\rho \Theta_i^{n+1}}, \tag{2e}$$

Trajectory equation

$$\mathbf{x}_r^{n+1} = \mathbf{x}_r^n + \Delta t \, \tilde{\mathbf{v}}_r^*. \tag{3}$$

Explicit numerical fluxes

Numerical fluxes for the heat conduction

$$\begin{aligned}
\widehat{\mathbf{q}_{fi} \cdot \mathbf{n}_{fi}} &= \frac{1}{2}\left((\alpha^2\theta\mathbf{J})_{fi} + (\alpha^2\theta\mathbf{J})_{fj}\right) \cdot \mathbf{n}_{fi} - \frac{1}{2}|\lambda_f|\left(E_{fj} - E_{fi}\right), \\
\widehat{\theta_{fi}\mathbb{I} \cdot \mathbf{n}_{fi}} &= \frac{1}{2}\left((\theta\mathbb{I})_{fi} + (\theta\mathbb{I})_{fj}\right) \cdot \mathbf{n}_{fi} - \frac{1}{2}|\lambda_f|\left(\mathbf{J}_{fj} - \mathbf{J}_{fi}\right),
\end{aligned}$$

with $\lambda_f = \max(a_i, a_j)$ and $a_i = \left.\sqrt{c_0^2 + \frac{4}{3}c_{\mathrm{sh}}^2 + c_{\mathrm{h}}^2}\,\right|_i$.

Discrete velocity gradient for the $\mathbb{G}_{e_i}$ equation

$$\mathbb{L}_i(\mathbf{v}) = \frac{1}{|T_i|}\sum_{r \in \mathcal{R}(i)} \mathbf{v}_r \otimes \mathbf{c}_{ri},$$

Nonlinear nodal solver

Subcell force balance (P.H. Maire, JCP 2009)

$$\mathbb{M}_r \tilde{\mathbf{v}}_r^* = \sum_{i \in \mathcal{T}_r} \mathbb{M}_{ir} \mathbf{v}_i^n - \mathbb{T}_i^* \mathbf{c}_{ri}^n$$

with the discrete subcell matrix $\mathbb{M}_{ir}$ and nodal matrix $\mathbb{M}_r$ given by

$$\mathbb{M}_{ir} = \sum_{f \in \mathcal{F}_{ri}} z_i^n \, s_f^n \, \mathbf{n}_f^n \otimes \mathbf{n}_f^n, \qquad \mathbb{M}_r = \sum_{i \in \mathcal{T}_r} \mathbb{M}_{ir}.$$

Subcell force definition: $\quad \tilde{\boldsymbol{f}}_{ri}^* = \mathbf{c}_{ri}^n \mathbb{T}_i^* + \mathbb{M}_{ir}(\tilde{\mathbf{v}}_r^* - \mathbf{v}_i^n)$

Implicit discretization for $\boldsymbol{\sigma}$: $\quad \boldsymbol{\sigma}_i^{n+1} = -\rho_i^{n+1} c_{\mathrm{sh}}^2 \, \mathbb{G}_{e_i}^{n+1} \, \mathring{\mathbb{G}}_{e_i}^{n+1}$

NB: the nodal solver must be coupled with the trajectory equation, the GCL and the equation for $\mathbb{G}_{e_i}$, in order to obtain $\mathbf{x}_r^{n+1}$, ρ_i^{n+1} and $\mathbb{G}_{e_i}^{n+1}$.

$$\Downarrow$$

strongly nonlinear system

Nonlinear nodal solver

Picard iterative solver for $l = 1, \dots, \mathcal{L}$

$$\tilde{\mathbf{v}}_r^{l+1,n+1} = \left(\sum_{i \in \mathcal{T}_r} \mathbb{M}_{ir} \mathbf{v}_i^n - \mathbb{T}_i^{l,n+1} \mathbf{c}_{ri}^n \right) \mathbb{M}_r^{-1},$$

$$\mathbf{x}_r^{l+1,n+1} = \mathbf{x}_r^n + \Delta t \, \tilde{\mathbf{v}}_r^{l+1,n+1},$$

$$\rho_i^{l+1,n+1} = \frac{m_i}{|T_i|^{l+1,n+1}},$$

$$\mathbb{G}_{e_i}^{l+1,n+1} = \mathbb{G}_{e_i}^n - \Delta t \left(\mathbb{G}_{e_i}^n \, \mathbb{L}_i(\tilde{\mathbf{v}}^{l+1,n+1}) + \mathbb{L}_i(\tilde{\mathbf{v}}^{l+1,n+1})^\top \, \mathbb{G}_{e_i}^n \right) + \Delta t \frac{2\sigma_i^{l+1,n+1}}{\rho^{l+1,n+1} \, \Theta_i^{l+1,n+1}},$$

$$\sigma_i^{l+1,n+1} = -\rho_i^{l+1,n+1} c_{\mathrm{sh}}^2 \, \mathbb{G}_{e_i}^{l+1,n+1} \, \mathring{\mathbb{G}}_{e_i}^{l+1,n+1}.$$

Fully implicit discretization for $\mathbb{G}_{e_i}^{l+1,n+1}$ *only*!

(Exponential integrator (W. Boscheri et al., JCP 2022))

Nonlinear nodal solver

Stopping criteria

- The material is an ideal gas → **hydrodynamics limit**

$$\epsilon_h^{l+1} := \left| \mathbb{G}_{e_i}^{l+1,n+1} - \left(\frac{\rho^{l+1,n+1}}{\rho_0} \right)^{2/3} \mathbb{I} \right| \leq \delta,$$

- The material is a purely elastic solid → **ideal elasticity limit**

$$\epsilon_e^{l+1} := \left| \mathbb{G}_{e_i}^{l+1,n+1} - \mathbb{G}_{i,*}^{l+1,n+1} \right| \leq \delta,$$

  where $\mathbb{G}_{i,*}^{l+1,n+1}$ is the solution of the homogeneous equation for $\mathbb{G}_{e_i}$.

- Convergence is achieved between two consecutive iterations for any of the following residuals (viscous flows and viscoplastic solids):

$$\left| \epsilon_h^{l+1} - \epsilon_h^{l} \right| \leq \delta, \qquad \left| \epsilon_e^{l+1} - \epsilon_e^{l} \right| \leq \delta.$$

Outline

Asymptotic preserving properties

Application of the Chapman-Enskog expansion

$$\phi = \phi_{(0)} + \varepsilon\phi_{(1)} + \varepsilon^2\phi_{(2)} + \ldots + \mathcal{O}(\varepsilon^k)$$

up to the first order in ε_2 and ε_1 to $\mathbf{J}_i$ and $\mathbb{G}_{e_i}$ yields

$$\begin{aligned}
\mathbf{J}_{i(0)}^{n+1} + \varepsilon_2 \mathbf{J}_{i(1)}^{n+1} - \mathbf{J}_{i(0)}^{n} - \varepsilon_2 \mathbf{J}_{i(1)}^{n} &= -\frac{\Delta t}{m_i} \sum_{f \in \mathcal{F}_i} \widehat{\theta_{fi}\mathbb{I} \cdot \mathbf{n}_{fi}}^{\,n} s_f^n - \frac{1}{\varepsilon_2}\frac{\theta_i^n}{\theta_0}\frac{\rho_0}{\rho_i^{n+1}} \left(\mathbf{J}_{i(0)}^{n+1} + \varepsilon_2 \mathbf{J}_{i(1)}^{n+1}\right) + \mathcal{O}(\varepsilon_2^2), \\
\mathbb{G}_{e_i(0)}^{n+1} + \varepsilon_1 \mathbb{G}_{e_i(1)}^{n+1} - \mathbb{G}_{e_i(0)}^{n} - \varepsilon_1 \mathbb{G}_{e_i(1)}^{n} &= -\Delta t \left[\left(\mathbb{G}_{e_i(0)}^{n} + \varepsilon_1 \mathbb{G}_{e_i(1)}^{n}\right) \mathbb{L}_i(\tilde{\mathbf{v}}^*) - \mathbb{L}_i(\tilde{\mathbf{v}}^*)^{\mathsf{T}} \left(\mathbb{G}_{e_i(0)}^{n} + \varepsilon_1 \mathbb{G}_{e_i(1)}^{n}\right)\right] \\
&\quad + \frac{6}{\varepsilon_1} \left|\mathbb{G}_{e_i(0)}^{n+1} + \varepsilon_1 \mathbb{G}_{e_i(1)}^{n+1}\right|^{5/6} \left(\mathbb{G}_{e_i(0)}^{n+1} + \varepsilon_1 \mathbb{G}_{e_i(1)}^{n+1}\right) \left(\mathring{\mathbb{G}}_{e_i(0)}^{n+1} + \varepsilon_1 \mathring{\mathbb{G}}_{e_i(1)}^{n+1}\right) \\
&\quad + \mathcal{O}(\varepsilon_1^2).
\end{aligned}$$

Asymptotic analysis

Heat flux limit of the at 1-st order	$\rightarrow$	discrete Fourier law
Viscous stress tensor limit at 0-th order	$\rightarrow$	discrete viscous stresses vanish
Viscous stress tensor limit at 1-st order	$\rightarrow$	discrete viscous stress of CNS

Outline

Space: TVD piecewise linear reconstruction

Reconstruction polynomial: $\mathbf{w}_i^n(\mathbf{x}^n) = \sum_{l=1}^{\mathcal{M}} \psi_l(\boldsymbol{\xi})\, \widehat{\mathbf{w}}_{l,i}^n$ (*modal* basis functions)

Reconstruction stencil: $\mathcal{S}_i = \bigcup_{j=1}^{n_e} T^n_{m(j)}$ with $n_e = d \cdot \mathcal{M}$

Conservation principle: $\frac{1}{|T_j^n|} \int\limits_{T_j^n} \psi_l(\boldsymbol{\xi}) \widehat{\mathbf{w}}_{l,i}^c \, \mathrm{d}\mathbf{x} = \mathbf{Q}_j^n, \qquad \forall T_j^n \in \mathcal{S}_i$

Minmod limiter: $\widehat{\mathbf{w}}_{l,i}^n = b_i \, \widehat{\mathbf{w}}_{l,i}^c \qquad \text{with} \qquad b_i = \min_{r \in \mathcal{R}_i} b_{i,r}$

$$b_{i,r} = \begin{cases} \min\left(1, \frac{\mathbf{Q}_i^{n,\max} - \mathbf{Q}_i^n}{\mathbf{w}_i^n(\mathbf{x}_r^n) - \mathbf{Q}_i^n}\right) & \text{if} \quad \mathbf{w}_i^n(\mathbf{x}_r^n) > \mathbf{Q}_i^n \\ \min\left(1, \frac{\mathbf{Q}_i^{n,\min} - \mathbf{Q}_i^n}{\mathbf{w}_i^n(\mathbf{x}_r^n) - \mathbf{Q}_i^n}\right) & \text{if} \quad \mathbf{w}_i^n(\mathbf{x}_r^n) < \mathbf{Q}_i^n \\ 1 & \text{if} \quad \mathbf{w}_i^n(\mathbf{x}_r^n) = \mathbf{Q}_i^n \end{cases}$$

Time: IMplicit-EXplicit Runge-Kutta time stepping

Splitting of the PDE: $\dfrac{\mathrm{d}\mathbf{Q}}{\mathrm{d}\,t} = \mathcal{L}_{ex}(t, \mathbf{Q}, \nabla \mathbf{Q}) + \mathcal{L}_{im}(t, \mathbf{Q})$

$$\mathcal{L}_{ex}(t, \mathbf{Q}, \nabla \mathbf{Q}) = \left[\begin{array}{c} \rho^{-1}\, \nabla \cdot \mathbf{v} \\ \rho^{-1}\, \nabla \cdot \mathbb{T} \\ \rho^{-1}\, \nabla \cdot (\mathbb{T}\mathbf{v} + \mathbf{q}) \\ \rho^{-1}\, \nabla \cdot T\, \mathbb{I} \\ -(\mathbb{G}_e \nabla \mathbf{v} + \nabla \mathbf{v}^{\top} \mathbb{G}_e) \end{array} \right], \qquad \mathcal{L}_{im}(t, \mathbf{Q}) = \left[\begin{array}{c} 0 \\ 0 \\ 0 \\ -\mathbf{H}/\Psi \\ 2\boldsymbol{\sigma}/(\rho\Theta) \end{array} \right].$$

Second order IMEX ARS(2,2,2) with $\beta = 1 - \sqrt{2}/2$

$$\begin{aligned} \frac{\mathbf{Q}^{(1)} - \mathbf{Q}^n}{\Delta t} &= \beta\, \mathcal{L}_{ex}(t^n, \mathbf{Q}^n, \nabla \mathbf{Q}^n) + \beta\, \mathcal{L}_{im}(t^{(1)}, \mathbf{Q}^{(1)}) \\ \frac{\mathbf{Q}^{n+1} - \mathbf{Q}^n}{\Delta t} &= (\beta - 1)\, \mathcal{L}_{ex}(t^n, \mathbf{Q}^n, \nabla \mathbf{Q}^n) + (2 - \beta)\, \mathcal{L}_{ex}(t^{(1)}, \mathbf{Q}^{(1)}, \nabla \mathbf{Q}^{(1)}) \\ &+ \beta \mathcal{L}_{im}(\mathbf{Q}^{(1)}) + (1 - \beta)\, \mathcal{L}_{im}(t^{(1)}, \mathbf{Q}^{(1)}) + \beta\, \mathcal{L}_{im}(t^{n+1}, \mathbf{Q}^{n+1}) \end{aligned}$$

Remark. The same discretization applies to the trajectory equation: $\dfrac{\mathrm{d}\mathbf{x}}{\mathrm{d}\,t} = \mathbf{v}$

Outline

Convergence studies (hydrodynamics limit: $\tau_1 = 10^{-14}$)

2D LGPR $\mathcal{O}1$ ($\tau_1 = 10^{-14}$)

$h(\Omega(t_f))$	$(\omega)_{L_2}$	$\mathcal{O}(1/\rho)$	u_{L_2}	$\mathcal{O}(u)$	E_{L_2}	$\mathcal{O}(E)$
3.26E-01	5.405E-02	-	1.547E-01	-	2.579E-01	-
2.47E-01	4.164E-02	0.96	1.219E-01	0.88	2.044E-01	0.86
1.63E-01	3.053E-02	0.74	8.866E-02	0.76	1.471E-01	0.78
1.28E-01	2.286E-02	1.20	7.041E-02	0.96	1.164E-01	0.97

2D LGPR $\mathcal{O}2$ ($\tau_1 = 10^{-14}$)

$h(\Omega(t_f))$	$(\omega)_{L_2}$	$\mathcal{O}(1/\rho)$	u_{L_2}	$\mathcal{O}(u)$	E_{L_2}	$\mathcal{O}(E)$
3.26E-01	4.996E-02	-	4.895E-02	-	9.281E-02	-
2.47E-01	3.312E-02	1.49	3.020E-02	1.76	5.509E-02	1.90
1.63E-01	1.913E-02	1.32	1.534E-02	1.63	2.858E-02	1.58
1.28E-01	1.327E-02	1.51	9.153E-03	2.13	1.770E-02	1.98

3D LGPR $\mathcal{O}1$ ($\tau_1 = 10^{-14}$)

$h(\Omega(t_f))$	$(\omega)_{L_2}$	$\mathcal{O}(1/\rho)$	u_{L_2}	$\mathcal{O}(u)$	E_{L_2}	$\mathcal{O}(E)$
5.29E-01	2.389E-01	-	5.600E-01	-	8.781E-01	-
3.62E-01	2.013E-01	0.35	4.075E-01	0.65	6.660E-01	0.56
2.31E-01	1.752E-01	0.31	2.882E-01	0.77	4.877E-01	0.69
1.81E-01	1.454E-01	0.76	2.301E-01	0.91	3.974E-01	0.83

3D LGPR $\mathcal{O}2$ ($\tau_1 = 10^{-14}$)

$h(\Omega(t_f))$	$(\omega)_{L_2}$	$\mathcal{O}(1/\rho)$	u_{L_2}	$\mathcal{O}(u)$	E_{L_2}	$\mathcal{O}(E)$
5.29E-01	2.899E-01	-	2.946E-01	-	5.185E-01	-
3.62E-01	1.426E-01	1.44	1.188E-01	1.85	2.275E-01	1.67
2.31E-01	8.304E-02	1.20	5.829E-02	1.59	1.099E-01	1.62
1.81E-01	5.931E-02	1.37	3.600E-02	1.96	7.206E-02	1.72

Kidder problem (hydrodynamics limit: $\tau_1 = 10^{-14}$)

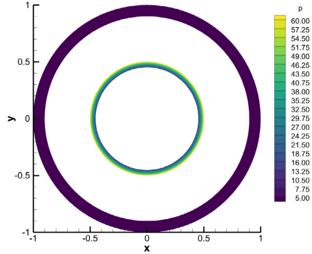

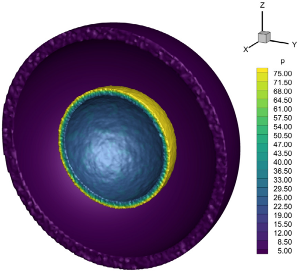

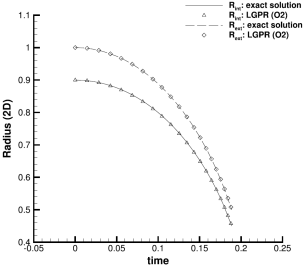

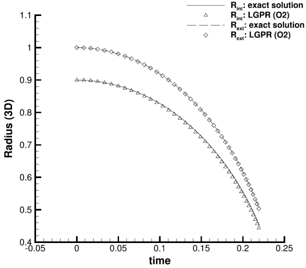

Sedov problem (hydrodynamics limit: $\tau_1 = 10^{-14}$)

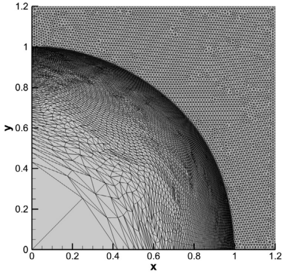

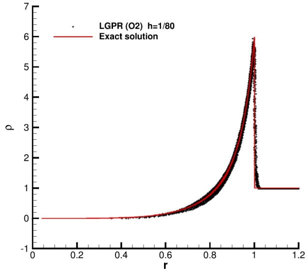

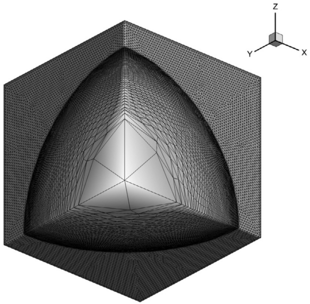

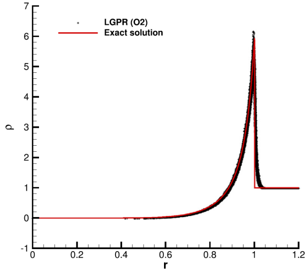

Riemann problems with viscous fluids ($\mu = \frac{1}{6}\rho_0\tau_1 c_{\rm sh}^2$)

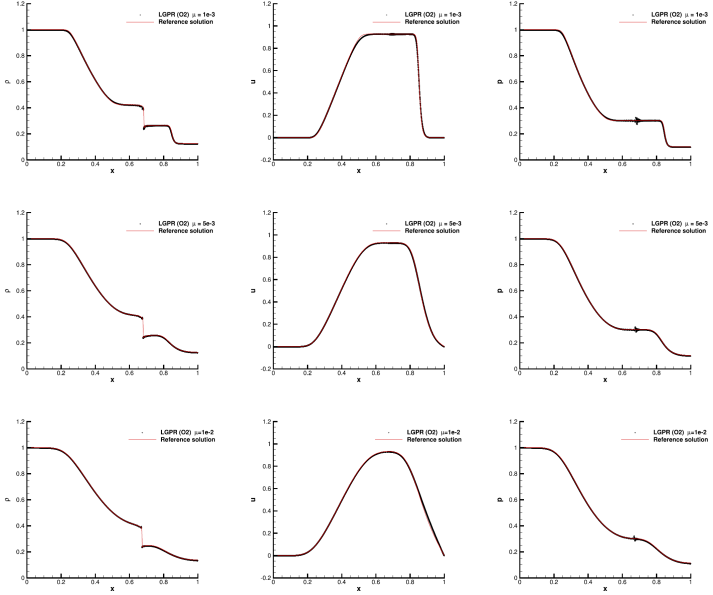

Heat conduction in a gas $(\kappa = \tau_2 \alpha^2 \frac{\theta_0}{\rho_0})$

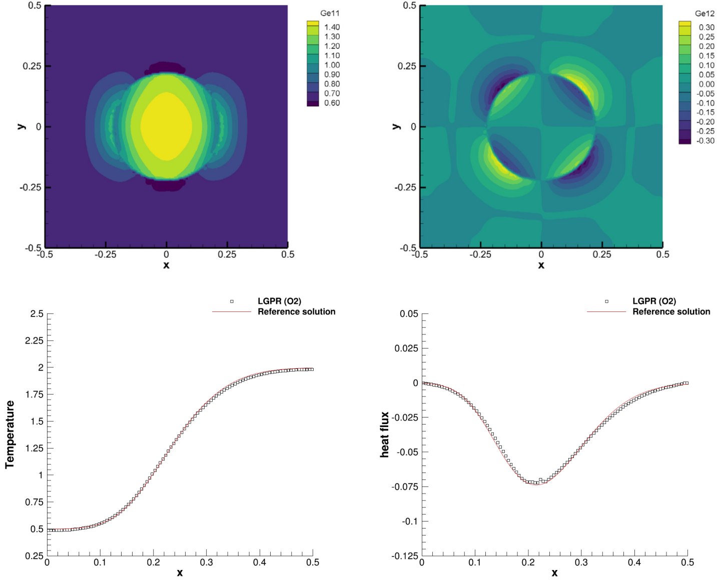

Collapse of a beryllium shell ($\tau_1 = \tau_{10}(\sigma_Y/\sigma)^n$)

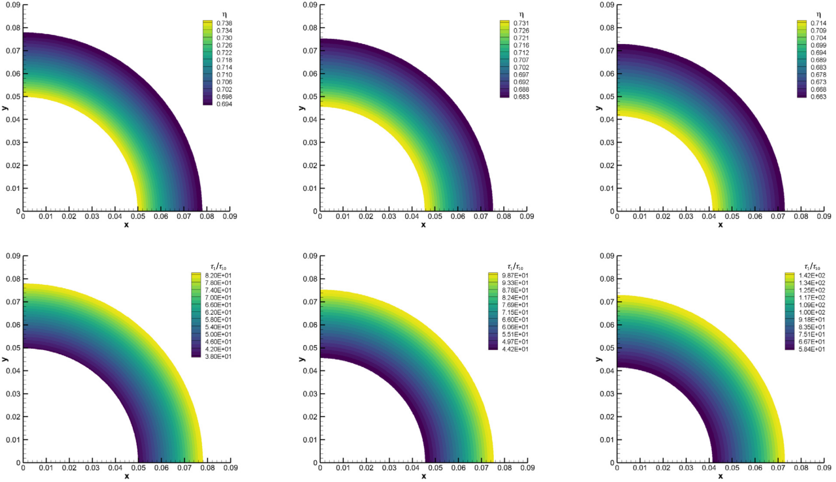

$V_0 = 417.1$ $\quad$ $V_0 = 454.7$ $\quad$ $V_0 = 490.2$

Collapse of a beryllium shell $(\tau_1 = \tau_{10}(\boldsymbol{\sigma}_Y/\boldsymbol{\sigma})^n)$

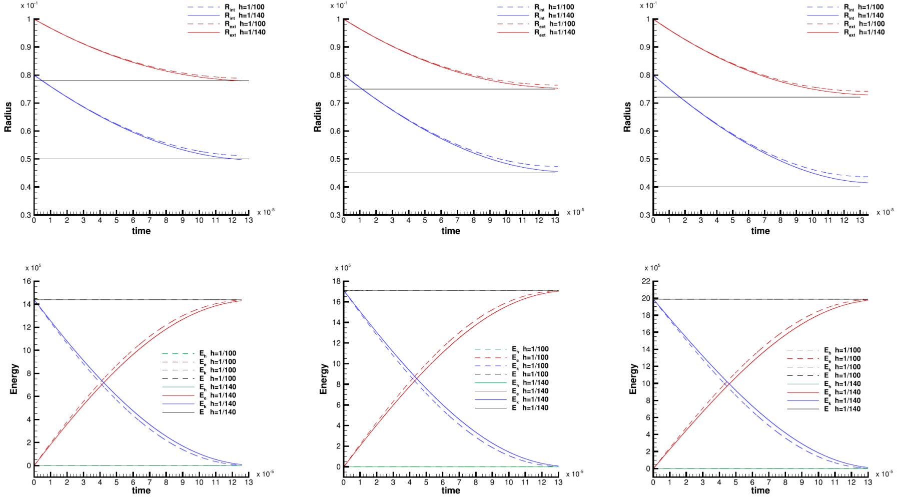

2D projectile impact $(\tau_1 = \tau_{10}(\boldsymbol{\sigma}_Y/\boldsymbol{\sigma})^n)$

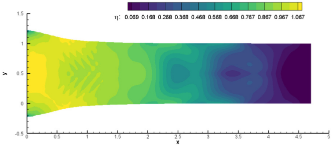

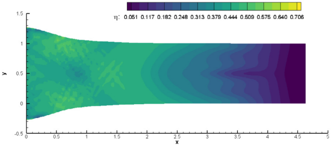

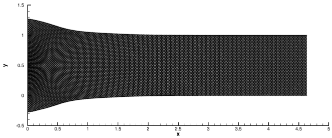

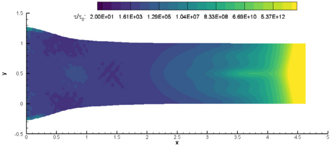

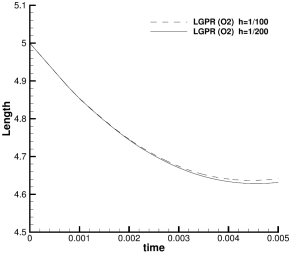

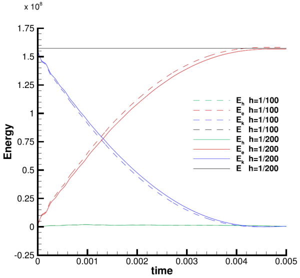

3D Taylor bar ($\tau_1 = \tau_{10}(\boldsymbol{\sigma}_Y/\boldsymbol{\sigma})^n$)

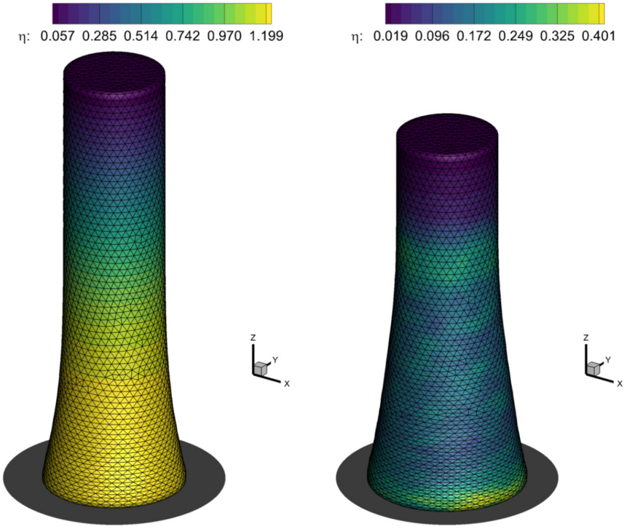

Plasticity map at time $t = 2 \cdot 10^{-5}$ and $t = 8 \cdot 10^{-5}$.

3D Taylor bar $(\tau_1 = \tau_{10}(\boldsymbol{\sigma}_Y/\boldsymbol{\sigma})^n)$

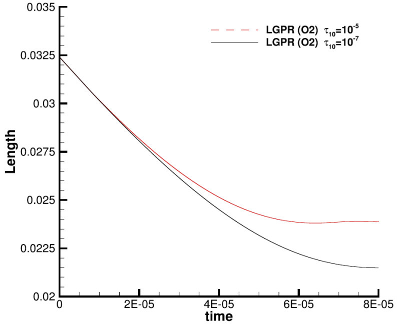

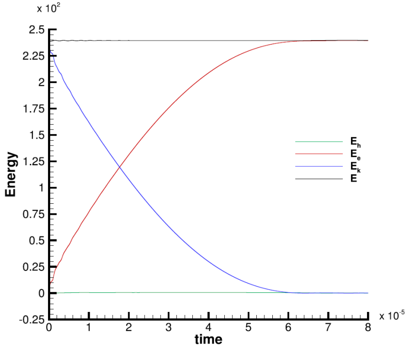

Elastic vibration of a beryllium plate (ideal elasticity: $\tau_1 = 10^{14}$)

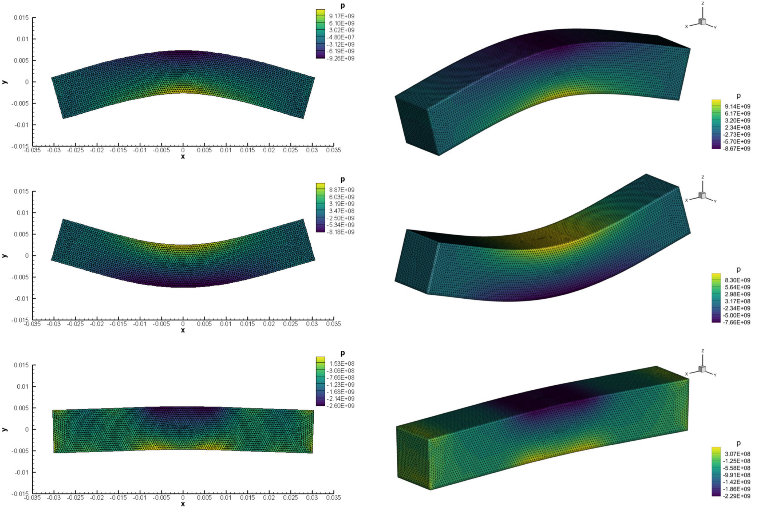

Elastic vibration of a beryllium plate (ideal elasticity: $\tau_1 = 10^{14}$)

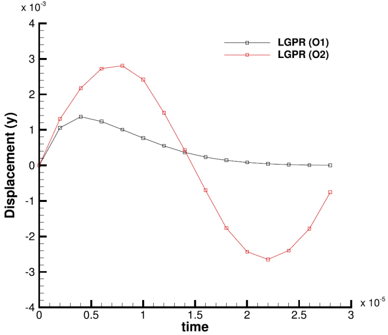

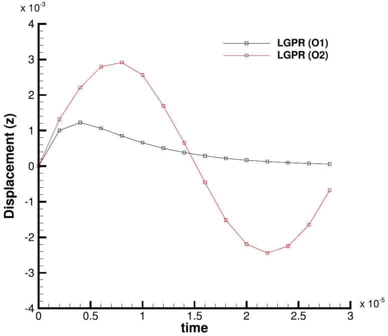

Twisting column (ideal elasticity: $\tau_1 = 10^{14}$)

Outline

Conclusions and Outlook

Conclusions

- a unified model for continuum mechanics in Lagrangian form
- new second order updated Lagrangian finite volume scheme for ideal and viscous heat conducting fluids and elastic and elasto-plastic solids
- solver for stiff relaxation source terms
- Implicit-Explicit (IMEX) scheme with Asymptotic Preserving property
- Geometric Conservation Law compliant discretization
- extended validation and verification test suite on unstructured 2D/3D meshes

Conclusions and Outlook

Outlook

- extension to high order of accuracy in space and time
- usage of curvilinear unstructured meshes
- structure-preserving Lagrangian schemes for involutive PDEs

Thank you!

walter.boscheri@unife.it

W. Boscheri, S. Chiocchetti, I. Peshkov. A cell-centered implicit-explicit Lagrangian scheme for a unified model of nonlinear continuum mechanics on unstructured meshes.
Journal of Computational Physics 451: 110852 (2022).